(1/3)

NSC92-2112-M009-034-
92　08　01　　　93　07　31

93　　5　　31

Introduction:

A dramatic colossal magnetoresistance (CMR) effects in the hole-doped manganites were discovered in 1990s [1-3]. The origins of CMR in perovskite-type manganites ($R_{1-x}A_xMnO_3$, where R being trivalent rare-earth element and A being divalent alkaline earth ions for hole-doped manganites) were widely investigated and the attention was focus on their rich phase diagram. In these compounds, the valence of manganese is a mixture of Mn^{3+} (t_{2g}^3 e_g^1) and Mn^{4+} (t_{2g}^3), in which double exchange (DE) mechanism [4-6] was inducted to describe the behavior of electrons in e_g orbital between Mn^{3+} and Mn^{4+}. The theoretical understanding is still fragmental, especially on intrinsic inhomogeneities [7], and the DE mechanism alone is failed to explain the transport properties of hole-doped manganites in high temperature region [8].

Motivation:

If the trivalent rare-earth atom is substituted by tetravalent cerium, the manganites will be converted into an electron-doped state and the valence states are driven in a mixture of Mn^{3+} (t_{2g}^3 e_g^1) and $Mn2+$ (t_{2g}^3 e_g^2) [9-14]. Because of the double exchange mechanism, operating between neighboring Mn^{3+}/Mn^{2+}, $La_{1-x}Ce_xMnO_3$ should own metal-insulator transition and ferromagnetism. Actually, $La_{0.7}Ce_{0.3}MnO_3$ (LCeMO) have a Tc of about 260 K, which is about the same to $La_{0.7}Ca_{0.3}MnO_3$ (LCMO), a good comparison between hole- and electron-doped manganites in transitional mechanism and phase segregation.

Review of Literatures:

The correlation between the electronic and magnetic properties of peroviskite manganites, and intrinsic inhomogeneities, has been studied by transmission electron microscope (TEM) [15, 16] measurements and scanning tunneling spectroscopy (STS) of scanning tunneling microscope (STM) [17-20]. Fäth *et al.* [17] observed the cloudlike patterns of $La_{0.7}Ca_{0.3}MnO_3$ in the scale of 10 nanometers just blew Curie temperature (T_c), which imply phase separation and electronic inhomogeneities. Renner *et al.* [20] showed charge ordering and phase separation in real space with atomic scale. These phenomena showed the significance of phase separation to CMR and metal-insulator transition, and implied incomplete theories and phase diagrams to prove out intrinsic inhomogeneities. Phase separation had been observed in many hole-doped manganites, and it seemed to be general for these compounds. The transportable carriers are both in e_g orbitals either the electron-doped or hole-doped manganites, so it inspires a doubt, "Is phase separation universal? ". The single-phase $La_{1-x}Ce_xMnO_3$ films make a good comparison possible between electron-doped and

hole-doped system.

Experiments:

Epitaxial films of LCeMO were grown on (100) $SrTiO_3$ substrate by pulsed laser deposition, using KrF (248 nm) excimer laser. The target was polycrystalline bulk and typically properties reported by previous literatures [9], and still in mixed-phase. Stoichiometric amounts of CeO_2, La_2O_3 (which had been preheated) and $MnCO_3$ powders were heated in air at 1100 ℃ for 20 hours then being ground, palletized, and sintered at 1400 ℃ for 27 hours and repeat again. To avoid mixed-phase situation, we varied the substrate temperature and laser energy density for optimal growth [21]. To acquire single phase LCeMO thin films, the substrate temperature was kept at 725 ℃ and oxygen pressure was controlled at 0.35 Torr. After deposition, the chamber was vented by oxygen and cooled down to room temperature. The film thickness was approximately 170 nm.

As shown in Fig. 1(a), the x-ray diffraction (XRD) of thin films is in single phase. The resistance and magnetization versus temperature (R-T and M-T) denote the metal-insulator transition (T_{MI}) and Curie temperature (T_c) are both about 260 K as shown in Fig. 1(b). The valance states of single-phase LCeMO films were investigated by C. Mitra et $al.$ [14], in which the results of x-ray absorption spectroscopy shown that all ions of this compound were in correct valence state. Our LCeMO films had also been checked in the same experiments. Hysteresis curves at 10 K, 100K and 200K denoted the coercive field and saturated field are about 5, 50, 200 Oe and 0.15 T, respectively, and is lower than the external field (0.35 Tesla) applied in STS measurements.
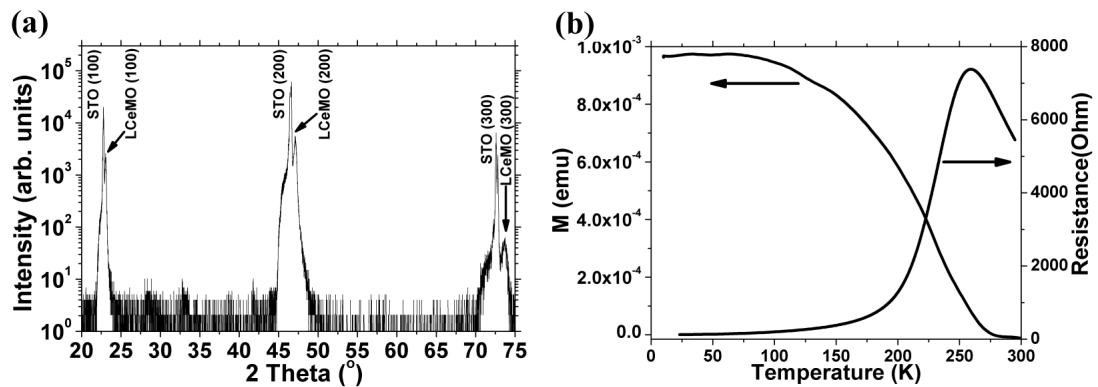
(a)

(b)

Figure 1

STM were used to obtain surface topographic and spectroscopic images at constant current mode with $Pt_{0.8}Ir_{0.2}$ tip. The sample was biased at 0.7 V relative to tip potential and the tunneling current was set at 0.5 nA. The lock-in amplifier was used

in the measurement of spectroscopic image as a standard lock-in technique [20]. The lock-in amplifier applied a small signal of sine wave on bias voltage (≤ 3%) and sensed the modulated tunneling current to output dI/dV data during scanning. STM was operated at a very slow scanning rate in measurements to improve the resolution of spectroscopic images, and the differential conductance (dI/dV) signal from lock-in amplifier were recorded with z-axis signal simultaneously. The I-V characteristics were scanned at each 16th point of STS with a voltage range from +1 V to –1 V. Fig. 2(c) illustrates the I-V characteristics of metallic phase (A curve) and insulating phase (B curve) at 80 K. The metallic states have a linearer I-V curve, compared to the I-V curves of insulating states, which leads to a smaller dI/dV value at the bias voltage 0.7 V, and being assigned on spectroscopic images as a dark region whereas the insulating states are assigned to the light regions of STS. Moreover, the contrast of spectroscopic images shows the relative intensity of every pixel, not absolute value between images. When choosing scanning area for STS, the maximum peak to peak depths of topography in spectroscopic images are smaller then 20nm [Fig. 2(a), (b)] in order to avoid turbulent tunneling current, which will show some components on the modulated frequency, and spectroscopic images sometimes depict insulating region along the sharp grain-boundaries.
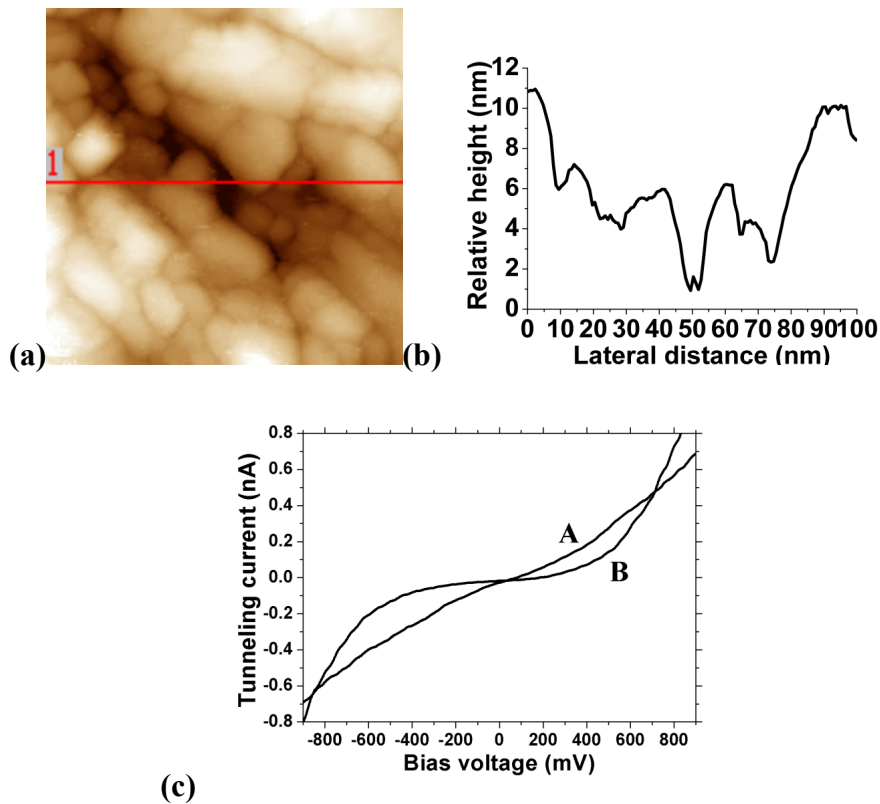

(a) (b)

(c)

Figure 2

Results and discussion:

We had measured STS over a wide temperature range which covers both side of the transition in 100×100 nm^2 area. Some steep relief of surface shut metallic phase in ravines even though applying 0.35 Tesla field. In most regions of surfaces, the metal-insulator separations were not directly relative to topography. At 300 K, there are small dark regions in spectroscopic images and they shift with applying magnetic field as shown in Fig. 3. Although the dark regions showed being more metallic to others, I-V characteristics were considerably non-linear at 300 K. The inhomogeneities of LCeMO were less perceptible at 300 K, comparing with the inhomogeneities below 230 K, and possessed a narrow dI/dV distribution [Fig.4] even if being applied magnetic field. Further more, the temperature was cool down to 230 K, a whole of LCeMO appear more metallic phase but the contrast of images was not vivid. After magnetic field was enhanced, dI/dV distribution [Fig. 4] shifted to metallic region (low dI/dV value) and the difference between metallic and insulating regions of spectroscopic image became visible. This is obviously to connect the enhanced hopping probability of e_g electrons, operated by DE mechanism, with the increase of metallic phase near T_c. The spectroscopic signature of LCMO displayed the patterns of insulating and metallic phase just blew T_c, as shown in the literature [17], but in the STS of LCeMO, the high contrast of metallic and insulating state revealed until cooling down to 200K, which was unlike the behavior of LCMO. The spectroscopic images at 80 K demonstrate the competition between metallic and insulating phase [Fig. 4]. The phase distribution was perturbed by an applied magnetic field of 0.35 T and the contrast of spectroscopic image became muddy. As shown in Fig. 5, the metallic state (~3.7 nA/V) move to insulating state let the phenomenon of phase separation blur out, and the average tunneling conductance are 7.172 nA/V and 7.268 nA/V for H=0 and H=0.35 T respectively. The results, comparing with the STS of at hillside of R-T curve (Metallic state was enhanced, average tunneling conductance from 8.297 nA/V to 7.986 nA/V, by adding external magnetic field at 230 K.), are very attractive. The insulating states increased in LCMO [17, 20] by applied magnetic field (~0.3 T), and the metallic states increased with magnetic field (> 1 T), which had been accepted intuitionally, but low field MR (LFMR) and high field MR (HFMR) are both negative. Obviously, the different mechanisms between HFMR and LFMR dominate the MR behavior of electron-doped and hole-doped manganites. There are still MR effects at low temperature, much below Tc and having achieved the maximum magnetization, whether hole- or electron-doped lanthanum manganites. If only DE mechanism dominates the ferromagnetic transition, the full ferromagnetism of whole manganites will not induce MR effects at low temperature. Additionally, M-T curves somehow sagged in low temperature region (< 50 K) and

R-T curves decrease with temperature below T_{MI}, but residual resistance was not zero as T→0. That may be due to spin-glasses phenomena or complex competition between FM and AFM.

In summary, we had measured the STS of LCeMO films from 300K to 80K. Beside similar R-T, M-T transition and e_g band majority spin carriers [21], the result showed that phase separation coexist in hole-doped and electron-doped compounds, which can be observed clearly in histogram of dI/dV distribution.
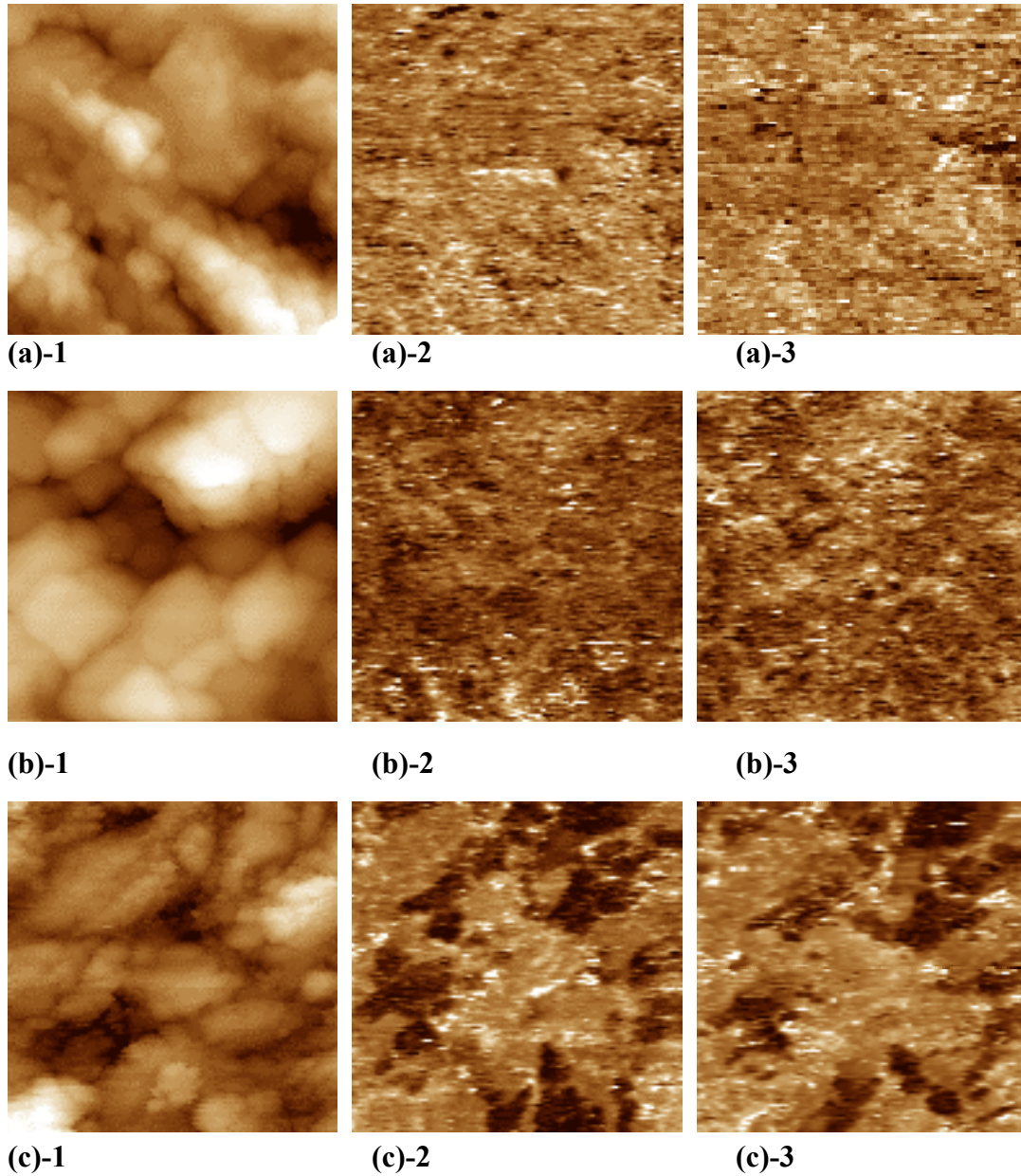

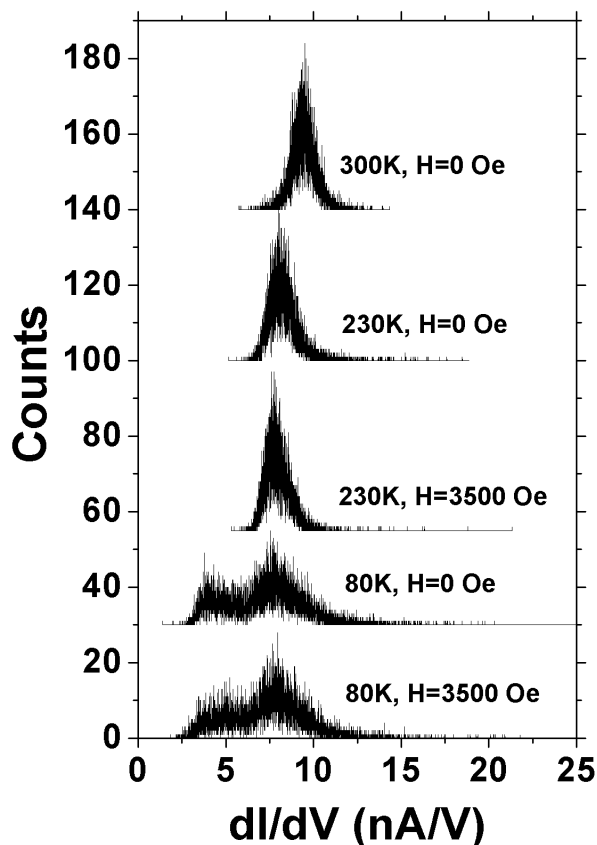**(a)-1**   **(a)-2**   **(a)-3**

(b)-1   **(b)-2**   **(b)-3**

(c)-1   **(c)-2**   **(c)-3**

Figure 3

Figure 4

Reference:

[1] P. Schiffer, A. P. Ramirez, W. Bao, S. -W. Cheong: Phys. Rev. Lett. **75**, 3336 (1995)

[2] A. Urushibara, Y. Moritomo, T. Arima et al.: Phys. Rev. B **51**, 14103 (1995)

[3] Y. Tomioka, A. Asamitsu, H. Kuwahara, and Y. Moritomo, and Y. Tokura: Phys. Rev. B **53**, R1689 (1996)

[4] C. Zener, Phys. Rev. **82**, 403 (1951)

[5] P. W. Anderson and H. Hasegawa, Phys. Rev. **100**, 675 (1955)

[6] P. -G. de Gennes, Phys. Rev. **118**, 141 (1960)

[7] *Nanoscale Phase Separation and Colossal Magnetoresistance / the physics of manganites and related compounds,* edited by Elbio Dagotto (Springer, 2003)

[8] A. J. Millis, P. B. Littlewood, and B. I. Shraiman, Phys. Rev. Lett. **74**, 5144 (1995)

[9] P. Mandal and S. Das, Phys. Rev. B **56**, 15073 (1997)

[10] John Philip and T R N Kutty, J. Phys.: Condens. Matter **11**,8537 (1999)

[11] P. Raychaudhuri, S. Mukherjee, A. K. Nigam, J. John, U. D. Vaisnav, R. Pinto and P. Mandal, J. Appl. Phys. **86**, 5718 (1999)

[12] J-S Kang, Y J Kim, B W Lee, C G Olson and B I Min, J. Phys.: Condens. Matter **13**,3779 (2001)

[13] C. Mitra, P. Raychaudhuri, K. Dörr, K. -H. Müller, L. Schultz, P.M. Oppeneer, and S.Wirth, Phys. Rev. Lett. **90**, 017202 (2003)

[14] C. Mitra, Z. Hu, P. Raychaudhuri, S. Wirth, S. I. Csiszar, H. H. Hsieh, H. -J. Lin, C. T. Chen, and L. H. Tjeng, Phys. Rev. B **67**, 092404 (2003)

[15] James C. Loudon, Nell D. Mathur and Paul A. Midgley, Nature **420**, 797 (2002)

[16] Y. Murakami, J. H. Yoo, D. Shindo, T. Atou and M. Kikuchi, Nature **423**, 965 (2003)

[17] M. Fäth, S. Freisem, A. A. Menovsky, Y. Tomioka, J. Aarts, J. A. Mydish, Science **285**, 1540 (1999)

[18] T. Becker, C. Streng, Y. Luo,V. Moshnyaga, B. Damaschke, N. Shannon and K. Samwer, Phys. Rev. Lett. **89**, 237203 (2002)

[19] Ch. Renner, G. Aeppli, B.-G. Kim, Yeong-Ah Soh and S.-W. Cheong, Nature **416**, 518 (2002)

[20] S. F. Chen, P. I. Lin, J. Y. Juang, T. M. Uen, K. H. Wu, Y. S. Gou and J. Y. Lin, Appl. Phys. Lett. 82, 1242 (2003)

[21] W. J. Chang *et al.* to be published.